Journal of Cerebral Blood Flow & Metabolism (2010) 30, 653–662

www.jcbfm.com

Effects of administration route on migration and distribution of neural progenitor cells transplanted into rats with focal cerebral ischemia, an MRI study

Lian Li[1], Quan Jiang[1], Guangliang Ding[1], Li Zhang[1], Zheng Gang Zhang[1], Qingjiang Li[1], Swayamprava Panda[1], Mei Lu[2], James R Ewing[1] and Michael Chopp[1,3]

[1]*Department of Neurology, Henry Ford Hospital, Detroit, Michigan, USA;* [2]*Department of Biostatistics and Research Epidemiology, Henry Ford Hospital, Detroit, Michigan, USA;* [3]*Department of Physics, Oakland University, Rochester, Michigan, USA*

We tested the hypotheses that administration routes affect the migration and distribution of grafted neural progenitor cells (NPCs) in the ischemic brain and that the ischemic lesion plays a role in mediating the grafting process. Male Wistar rats ($n = 41$) were subjected to 2-h middle cerebral artery occlusion (MCAo), followed 1 day later by administration of magnetically labeled NPCs. Rats with MCAo were assigned to one of three treatment groups targeted for cell transplantation intra-arterially (IA), intracisternally (IC), or intravenously (IV). MRI measurements consisting of T2-weighted imaging and three-dimensional (3D) gradient echo imaging were performed 24 h after MCAo, 4 h after cell injection, and once a day for 4 days. Prussian blue staining was used to identify the labeled cells, 3D MRI to detect cell migration and distribution, and T2 map to assess lesion volumes. Intra-arterial (IA) administration showed significantly increased migration, a far more diffuse distribution pattern, and a larger number of transplanted NPCs in the target brain than IC or IV administration. However, high mortality with IA delivery (IA: 41%; IC: 17%; IV: 8%) poses a serious concern for using this route of administration. Animals with smaller lesions at the time of transplantation have fewer grafted cells in the parenchyma.
Journal of Cerebral Blood Flow & Metabolism (2010) **30,** 653–662; doi:10.1038/jcbfm.2009.238; published online 4 November 2009

Keywords: administration route; lesion volume; MRI; neural progenitor cell; rat; transient ischemia

Introduction

Transplantation of neural progenitor cells (NPCs) following experimental stroke has been shown to improve functional recovery (Ishibashi *et al*, 2004; Jiang *et al*, 2006; Mochizuki *et al*, 2008). The likely mechanisms associated with functional improvement have been suggested to result from the ability of the grafted cells to reduce apoptosis (Chen *et al*, 2003*a*) and brain atrophy (Chu *et al*, 2004; Mochizuki *et al*, 2008; Chen *et al*, 2008), enhance angiogenesis (Chen *et al*, 2003*b*), release neurotrophic factors (Li *et al*, 2002; Ishibashi *et al*, 2004; Garcia *et al*, 2004), differentiate into other cells (Zhao *et al*, 2002; Chen *et al*, 2008), and promote endogenous cell proliferation (Chen *et al*, 2003*a*) and axonal remodeling (Jiang *et al*, 2006; Li *et al*, 2006; Shen *et al*, 2006). Therapeutic benefits gained from cell-based therapy depend on migration and localization of grafted cells within the target tissue (Modo *et al*, 2002; Savitz *et al*, 2004; Mochizuki *et al*, 2008), which can be non-invasively and dynamically detected by magnetic resonance imaging (MRI) (Heohn *et al*, 2002; Zhang *et al*, 2004; Magnitsky *et al*, 2005; Arbab *et al*, 2006; Walczak *et al*, 2008). Being able to track the magnetically labeled cells *in vivo*, MRI can provide longitudinal information regarding migratory capacity, homing potential, distribution pattern, and amount of the grafted cells present in the tissue, which are closely related to the therapeutic efficacy.

The cell delivery route chosen for the therapy may influence the migration and final destination of the transplanted cells. The cells can be precisely injected into the ischemic brain adjacent to the lesion area

Correspondence: Dr Q Jiang, B126, Education & Research Building, Department of Neurology, Henry Ford Hospital, 2799 West Grand Boulevard, Detroit, MI 48202, USA.
E-mail: QJIANG1@hfhs.org
This work was supported by National Institute of Neurological Diseases and Stroke grants P50 NS23393, PO1 NS42345, RO1 NS48349, RO1 NS38292, RO1 NS43324, and HL64766, and the Mort and Brigitte Harris Foundation.
Received 7 August 2009; revised 28 September 2009; accepted 19 October 2009; published online 4 November 2009

without loss (Chen *et al*, 2000; Zhao *et al*, 2002; Chen *et al*, 2008) or into the vascular system, for example, vein (Chen *et al*, 2001, 2003*a*, *b*; Chu *et al*, 2004), far away from target tissue, leading some cells to be trapped in systemic organs (Chopp and Li, 2002; Chu *et al*, 2004; Kraitchman *et al*, 2005; Hauger *et al*, 2006; Parr *et al*, 2007). In previous experimental studies, various cell delivery routes, such as introducing cells intravenously (Chen *et al*, 2001, 2003*a*, *b*; Chu *et al*, 2004), intra-arterially (Li *et al*, 2001; Shen *et al*, 2006; Walczak *et al*, 2008), intracisternally (Zhang *et al*, 2004), intraperitoneally (Gao *et al*, 2001), intraventricularly (Ohta *et al*, 2004), intracerebrally (Chen *et al*, 2000; Zhao *et al*, 2002; Ishibashi *et al*, 2004; Chen *et al*, 2008), or even directly into the lesion site (Amsalem *et al*, 2007), have been adopted to investigate therapeutic benefit and mechanisms involved. However, it remains unclear how the route of cell administration affects the grafting process in terms of migration, distribution, and numbers of cells in the target tissue, which in turn may determine the therapeutic efficacy. In addition, the grafting process may be mediated by the status of ischemic brain, such as stroke severity at the time of treatment because, the tissue injury induces cell migration to the site of damage (Chopp and Li, 2002; Heohn *et al*, 2002; Shyu *et al*, 2006). But to our knowledge, how the relationship between the extent of ischemic injury and the presence of exogenously administrated cells in the brain has not been investigated. Clarification of these issues may be important for optimization of treatment protocol and selection of subjects who might benefit from the therapy. In this study, we investigated the effects of intra-arterial (IA), intracisternal (IC), and intravenous (IV) injection on migration and distribution of transplanted NPCs in the living rat parenchyma using MRI. We also investigated the interaction between cell grafting and volume of cerebral infarction.

Materials and methods

All experimental procedures were approved and conducted in accordance with the institutional guidelines for care and use of laboratory animals.

Neurosphere Culture and Cell Labeling

NPCs were dissociated from the subventricular zone of normal male Wistar rats (Jackson Laboratory, Bar Harbor, ME, USA) aged 3 to 4 months, as previously reported (Luskin *et al*, 1997). These subventricular zone cells have been shown to have characteristics of neural progenitor cells (Liu *et al*, 2007). The cells were suspended at a density of 10,000 to 20,000 cells per milliliter in serum-free growth medium containing Dulbecco's modified Eagle's-F-12 medium (DMEM; Invitrogen Corporation, Carlsbad, CA, USA), 20 ng/ml of epidermal growth factor (R&D Systems, Minneapolis, MN, USA), and 20 ng/ml of basic fibroblast growth factor (R&D Systems). The generated neurospheres (primary sphere) were passaged by mechanical dissociation and reseeded as single cells at a density of 20 cells per microliter in basic fibroblast growth factor- and epidermal growth factor-containing media. Passage-1 cells were used in this study.

Cells were labeled *in vitro* with superparamagnetic iron oxide (SPIO) nanoparticles (Magnitsky *et al*, 2005; Amsalem *et al*, 2007). The commercially available ferumoxide suspension (Feridex IV; Berlex Laboratories, Wayne, NJ, USA) and protamine sulfate (American Pharmaceuticals Partner, Schaumburg, IL, USA) were used to generate ferumoxide–protamine sulfate (Fe–Pro) complexes (Arbab *et al*, 2004). Protamine sulfate was prepared as a fresh stock solution of 1 mg/ml in distilled water at the time of use. Serum-free medium, ferumoxide suspension, and protamine sulfate at a ratio of 1 ml:100 μg:5 μg were mixed in a flask for 5 to 10 min with intermittent hand shakings. Old medium in cell culture was replaced by this solution containing Fe–Pro complexes and the cells were incubated in the solution for 2 h. Then, complete medium was added to obtain a final concentration of 50 μg/ml for ferumoxide and 2.5 μg/ml for protamine sulfate, respectively. The cell suspension was incubated overnight at 37°C in a 5% CO_2 humidified atmosphere. Before injection into rats, the labeled cells were suspended in phosphate-buffered saline (PBS).

The viability of the SPIO-labeled NPCs before transplantation was assessed by trypan blue exclusion assay (Amsalem *et al*, 2007) and the tests showed that more than 95% of the cells remained viable after labeling with SPIO.

Animal Model and Cell Transplantation Procedures

Male Wistar rats (300 to 350 g, $n = 41$) were subjected to 2-h intraluminal middle cerebral artery occlusion (MCAo), followed 1 day later by administration of NPCs labeled with SPIO.

Rats were anesthetized with 3.5% halothane for induction and maintained by spontaneously respired 1.0% halothane in a 2:1 N_2O:O_2 mixture using a face mask. The rectal temperature was kept at 37°C ± 1°C throughout the surgical procedure using a feedback-regulated water-heating system. MCAo was induced by advancing a 4-0 surgical nylon suture, with its tip rounded by heating near a flame, from the external carotid artery into the lumen of internal carotid artery (ICA) to block the origin of right middle cerebral artery (MCA). After 2 h of MCAo, reperfusion was achieved by withdrawing the endovascular suture to the stump of the external carotid artery. The procedure provides a focal infarct in the unilateral striatum and cortex.

Rats subjected to transient MCAo were randomized to one of three treatment groups targeted for cell transplantation intra-arterially (carotid artery, $n = 17$) (Li *et al*, 2001; Shen *et al*, 2006), intracisternally (cisterna magna, $n = 12$) (Zhang *et al*, 2004), or intravenously (tail vein, $n = 12$) (Chen *et al*, 2003*a*; Chen *et al*, 2003*b*). Due to high mortality coming with carotid artery injection (Walczak *et al*, 2008), more animals were assigned to the IA than the IV and IC group. Anesthesia was reinstituted before

transplantation and a bolus of the cell suspension was slowly injected over a 5-min period into each rat using a Hamilton syringe (approximately 1×10^5 NPCs in 10 μl PBS for IC injection; 1×10^6 NPCs in 1 ml PBS for IA and IV injection). The needle was left in place for 1 min before withdrawal to minimize cell leakage and the injection site was compressed for a short time to reduce bleeding. No immunosuppressants were used in this study.

MR Imaging and Data Processing

MR imaging was performed using a 7 T, 20-cm-bore, superconducting magnet (Magnex Scientific, Abingdon, UK) interfaced to a Bruker console (Bruker, Boston, MA, USA). The animal was placed on a non-magnetic holder equipped with a nose cone for administration of anesthetic gases and stereotaxic ear bars to minimize movement of the head. A tri-pilot scan of imaging sequence was used for reproducible positioning of the animal in the magnet at each MRI session. During the imaging procedure, anesthesia was maintained with 1.0% halothane in 69% N_2O and 30% O_2, and rectal temperature was kept at $37^{\circ}C \pm 1.0^{\circ}C$ using a feedback-controlled water bath. *In vivo* T2-weighted imaging (T2WI) and high-resolution three-dimensional (3D) gradient echo imaging were performed for all animals 24 h after MCAo (before cell injection), 4 h after cell injection, and once a day for 4 days (Figure 1). All rats were killed after the final *in vivo* MRI scans (4 days after cell transplantation) followed by *ex vivo* MRI measurements.

In vivo MR Imaging

T2WIs were acquired using standard two-dimensional Fourier-transform, multi-slice (13 slices, 1 mm thick), multi-echo (six echoes) MRI. Six sets of images (13 slices per set) were obtained using echo times (TEs) of 15, 30, 45, 60, 75, and 90 ms, and a repetition time (TR) of 8 secs. Images were produced using a 32×32-mm^2 field of view and a 128×64 image matrix. The total sequence time was approximately 9 min.

3D gradient echo images were acquired with TR of 40 ms, TE of 10 ms, flip angle of 30 degrees, and a $32 \times 32 \times 24$-mm^3 field of view. The $256 \times 192 \times 64$ image matrix was interpolated to $256 \times 256 \times 64$ for analysis.

Ex Vivo MR Imaging

Perfusion-fixed rat brains were removed and immersed in Fomblin (Thorofare, NJ, USA). High-resolution *ex vivo* 3D MRI was obtained with TR of 40 ms, TE of 10 ms, flip angle of 30 degrees, a $32 \times 32 \times 24$-mm^3 field of view, and a $256 \times 256 \times 128$ image matrix.

MRI Data Processing

The ischemic lesion was identified on a T2 map (Figures 2A–2C). The lesion area on each slice of T2 map was specified by those pixels with a T2 value higher than the mean plus twice the standard deviation (mean + 2s.d.) provided by the normal tissue on the contralateral (non-ischemic) side (Li *et al*, 2005). Lesion volume was then calculated on the basis of lesion areas on individual slices and slice thickness. Data are presented as percentage of brain volume. Lesion reduction after cell administration, the difference in lesion volume between the day of cell transplantation and 4 days after cell transplantation, was also calculated and presented as percentage of lesion volume on the day of cell injection.

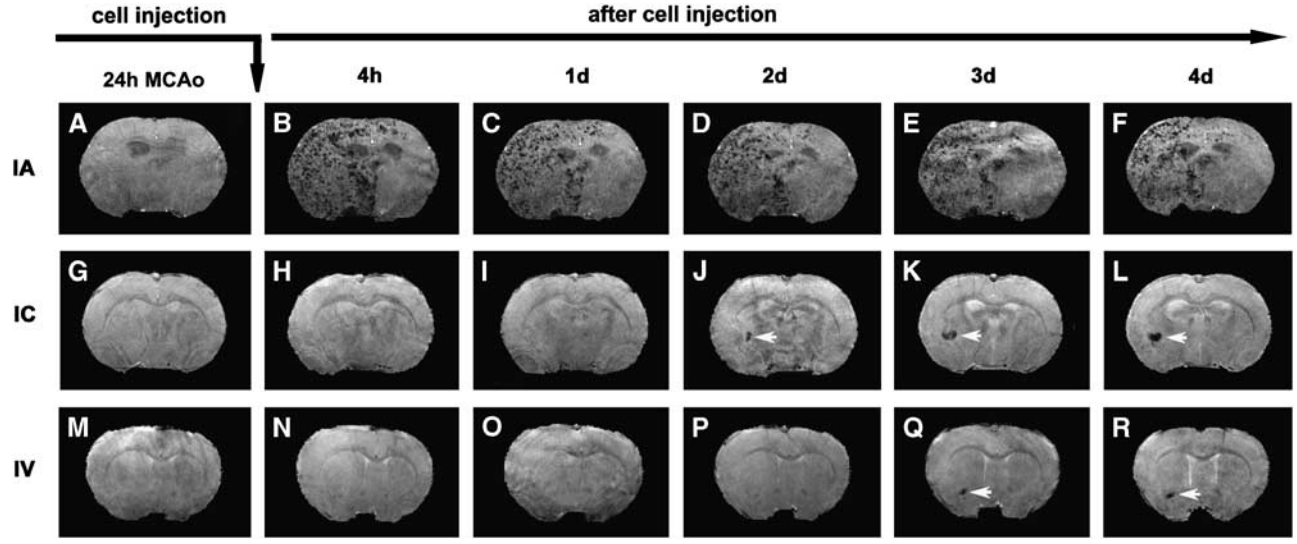

Figure 1 Consecutive 3D images of representative animals showing the dynamic evolution of migration, distribution, and amount of SPIO-labeled NPCs in the host brain after IA (top row), IC (middle row), and IV (bottom row) administration after transient MCAo. The ischemic lesions were located on the right side of the brain (the left side of the images). While the cells could be detected as soon as 4 h after IA injection (**B**), they were not seen until 2 days after IC (**J**) or 3 days after IV (**Q**) injection. Transplanted NPCs could distribute in a wide range in the ipsilateral side of the brain after IA administration (**B** to **F**). In contrast, the cells usually congregated in a limited area in the ipsilateral side after IC (white arrows, **J** to **L**) and IV (white arrows, **Q** and **R**) administration.

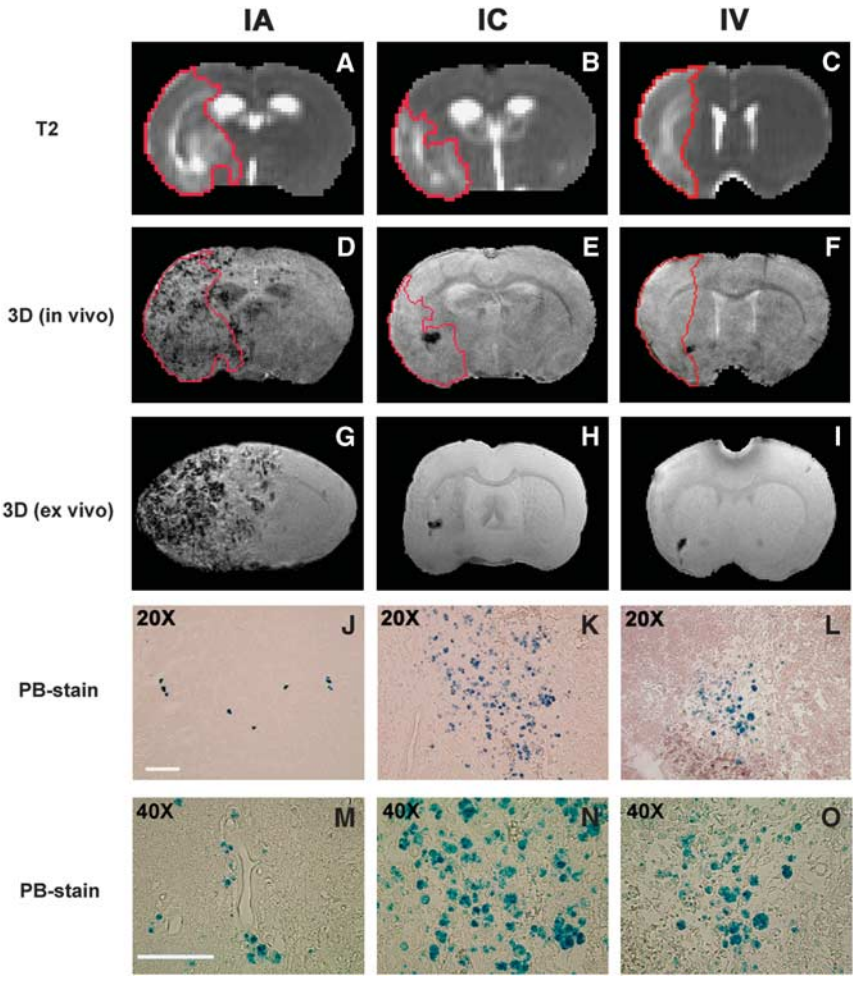

Figure 2 The distribution pattern of grafted NPCs in the host brain and the relationship between ischemic lesion and cell localization 4 days after IA (left column), IC (middle column), and IV (right column) administration. Lesion areas were identified on T2 maps (**A** to **C**, red tracks). SPIO-labeled NPCs resulted in signal reduction on *in vivo* 3D MRIs (**D** to **F**), which were confirmed by *ex vivo* 3D MRIs (**G** to **I**) and corresponding PB-stained sections (**J** to **L**). Due to the difference in slice thickness between MRI images and histological sections, the areas of PB-positive cells on the tissue section appears less than the areas of signal reduction on MRI images, particularly for IA group (**J**). Transplanted NPCs could scatter discretely throughout the entire lesion area in the ipsilateral side of the brain after IA administration (**D**), whereas the typical pattern after IC and IV administration was characterized by the cell clusters with numerous NPCs (**K** and **L**) congregating somewhere nearby lesion boundary or adjacent to healthier tissue (**E** and **F**). The PB-positive cells were found within the brain parenchyma 4 days after transplantation for three delivery routes (**M** to **O**). The representative animals shown here had similar lesion volume (presented as percentage of brain volume) at the time of cell transplantation: 33%, 37%, and 34% for animals with IA (left column), IC (middle column), and IV (right column) delivery, respectively. Scale bar (shown in panels **J** and **M**) = 100μm.

SPIO-labeled NPCs in the host brain resulted in dramatic signal reduction on 3D images, producing a strong contrast against the non-cell tissue background as shown in Figures 1 and 2. These hypo-intense areas on each slice of 3D images were specified by those pixels with signal intensity lower than the mean minus twice the standard deviation (mean−2s.d.) measured from non-cell tissue area on the contralateral side. Similarly, the volume of signal reduction for each animal was calculated from the hypo-intense areas identified on individual slices and slice thickness of 3D images. More labeled NPCs would induce a larger volume of signal loss on 3D images.

Tissue Preparation and Histology

Immediately after the final *in vivo* MRI measurements at 4 days after cell transplantation, rats were deeply anesthetized with ketamine (44 mg/kg, intraperitoneal) and xylazine (13 mg/kg, intraperitoneal), and transcardially perfused with heparinized saline followed by 4% paraformaldehyde. The brains were removed shortly after death and prepared for *ex vivo* experiments, as described above. At the end of the *ex vivo* MRI scans, the brains were rinsed with PBS solution, placed in 4% paraformaldehyde in PBS at 4°C for 2 days, and then cut into seven contiguous, 2-mm thick coronal blocks. Coronal sections

6 μm thick were sliced from each block embedded in paraffin and stained for histological evaluation.

To detect labeled NPCs in the host brain, tissue sections were stained for iron using Prussian blue (PB) reaction (Jiang *et al*, 2006). The coronal tissue sections were deparaffinized, rinsed in deionized water, and incubated for 30 min with 2% potassium ferrocyanide (Perls' reagent) in 6% HCl, and then washed well with distilled water and counterstained with nuclear fast red.

Microscopic observation and analysis were performed using a 3-CCD color video camera (Sony DXC-970MD; Ampronix Inc., Irvine, CA, USA) interfaced with a MicroComputer Imaging Device (MCID) system (Imaging Research Inc., St Catherines, ON, Canada).

Statistical Analysis

χ^2-test/exact test was employed to compare the mortality due to cell delivery among treatment groups. The Kaplan–Meier approach was used to test the group difference in time point for grafted NPCs being detected in the host brain, using the log-rank test with the estimated median time (the time at which grafted cells were detected in 50% of subjects studied). One-way or two-way analysis of variance was used to compare the volume of SPIO-induced signal reduction, the lesion volume, and lesion reduction between treatment groups and between groups with more and fewer cells. Analysis began with testing the overall route effect, followed by pairwise comparisons if the effect was significant at 0.05 level. Correlative analysis was performed between lesion volume on the day of cell transplantation and volume of SPIO-induced signal reduction on 3D MRI 4 days after transplantation. The measurement results are summarized as mean $\pm$ s.e. Statistical significance was inferred for $P \leq 0.05$.

Results

MRI Detection of Transplanted NPCs

Areas of signal intensity decrease on *in vivo* 3D MRI were observed after cell transplantation and the timing of these events depended on the delivery route (Figure 1). Numerous focal areas of low signal intensity on the ischemic side of the brain presented soon after IA administration (Figure 1B), while local spots of signal loss were observed later after IC and IV administration (Figures 1J and 1Q, white arrows). In contrast, these areas with decreased signal intensity were absent before the cell transplantation for all delivery routes (Figures 1A, 1G, and 1M), and typically 1 day (Figures 1H and 1I) and 2 days (Figures 1N–1P) after cell transplantation for IC and IV delivery, respectively. Whenever these hypo-intense areas appeared, they were persistently detected *in vivo* (Figures 1B–1F; Figures 1J–1L; and Figures 1Q and 1R) and further confirmed *ex vivo* (comparing Figures 2D–2F with Figures 2G–2I).

Success of cell engraftment in target brain was examined by histology. Histological evaluation of PB-stained tissue sections showed that SPIO-labeled NPCs transplanted through IA, IC, and IV delivery routes following stroke arrived at the ischemia-injured brain. The cellular distribution in the host brain was represented by PB-positive material inside the engrafted NPCs (blue spots; Figures 2J–2L), indicative of the presence of iron that was used for labeling the cells. The PB-positive cells were found within the brain parenchyma 4 days after transplantation for three delivery routes, as shown by micrographs at higher magnification (Figures 2M–2O).

Comparison between 3D images and the corresponding PB-stained tissue sections showed that the hypo-intense site seen on 3D MRI coincided with the histological location of the iron-positive area for all animals (Figure 2). This spatial colocalization between cell identification on tissue slices and appearance of signal damping on MRI images indicates that SPIO-labeled NPCs can be visualized *in vivo* on 3D MRI as a strong signal reduction. The hypo-intense areas detected at an earlier stage after IA transplantation, such as 4 h after injection (Figure 1B), may represent the distribution of labeled NPCs in the blood vessels. But for all three delivery routes, the pattern with reduced signal on 3D MRI 4 days after transplantation results from grafted cells in the brain parenchyma (Figures 2M–2O).

Migration and Distribution of Transplanted NPCs

With all three delivery routes, both histological evaluation and MR imaging showed that most of the transplanted NPCs were located on the ischemic side of the brain, with very few on the contralateral side. On the ischemic side, cells were located in the lesion core and the border region between intact normal tissue and the area of infarction. Using T2 map to identify the ischemic lesion (Figures 2A–2C), the cells were detected within and surrounding the lesion area (Figures 2D–2F). As shown in Figure 2, the cell administration route remarkably affected the final pattern of cellular distribution in the host brain, even though the treated animals had a similar degree of ischemic injury (such as lesion volume) at the time of cell transplantation. Transplanted NPCs scattered discretely (as small clusters of cells; Figure 2J) throughout the entire lesion area on the ipsilateral side of the brain after IA administration (Figure 2D), whereas the typical cellular distribution pattern after IC and IV administration was characterized by the cell clusters with numerous NPCs (Figures 2K and 2L) congregating somewhere nearby the lesion boundary or adjacent to healthier tissue (Figures 2E and 2F). PB-stained tissue sections showed that after IC and IV administration, most NPCs entering the brain gathered in these cluster areas (with very few in the other site), which were readily detected by 3D MRI

(Figures 1J–1L; Figures 1Q and 1R). Notably, while labeled NPCs could be detected as soon as 4 h after IA injection (Figure 1B), they were not seen until 1 to 2 days after IC (Figure 1J, white arrow), or 2 to 3 days after IV (Figure 1G, white arrow) injection. Statistical analysis showed that the time points for NPCs being detected in the brain were significantly different among the three treatment groups (overall route effect, $P<0.01$). The estimated median time was 4 h after IA, as compared with 2 days after IC ($P=0.05$) and 3 days after IV ($P<0.05$) administration, respectively. When using the volume of SPIO-induced signal reduction on 3D MRI (4 days after injection) to roughly assess the amount of cells detected in the host brain, we found that for the same stroke model, IA delivery led to the largest amount of grafted cells, followed by IC and IV delivery, respectively. These data indicate that IA delivery results in earlier engraftment, more uniform and widespread distribution, and a larger number of transplanted cells in the host brain than IC or IV delivery.

Lesion Volume and NPCs in the Host Brain

As described above, NPCs migrated into the ischemic brain after IA, IC, and IV administration. The amount of cells present in the host brain, as measured by hypo-intense pixels on 3D MRI, varied from group to group and from animal to animal even through the same administration route. However, we found two distinct clusters of pixels with hypo-intensity in all treatment groups, low and high, with no intermediate value. For the IA group, the total number of pixels with hypo-intensity on 3D images was either <8 ($n=2$) or >200 ($n=4$). For the IC and IV group, the low and high clusters were <20 ($n=2$) and 10 ($n=3$) or >120 ($n=6$) and 90 ($n=6$), respectively. We, therefore, used 0.12 mm^3 (20 pixels) of SPIO-induced signal reduction on 3D MRI as a threshold to divide the animals into groups with fewer or more cells. In each treatment group, a smaller lesion volume on the day of cell transplantation corresponded to fewer cells detected in the brain 4 days after transplantation (Figure 3C) (no difference in lesion volume on

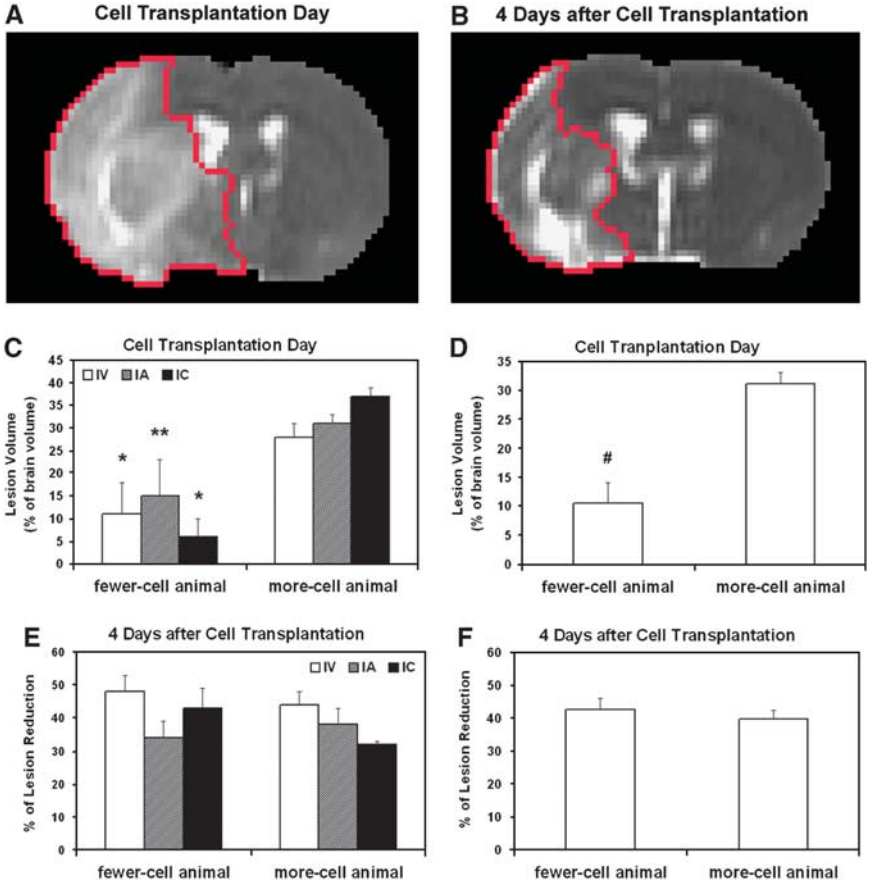

Figure 3 Lesion reduction after cell transplantation presented by the same slices of T2 maps at two time points (red tracks in panels **A** and **B**) and quantitative data of lesion volume (**C** and **D**) and lesion reduction (**E** and **F**) for more- and fewer-cell animals. For each treatment group, a smaller lesion volume on the day of cell transplantation corresponded to fewer cells detected in the brain 4 days after transplantation (**C**, $*P<0.04$; $**P=0.09$, fewer-cell animal versus more-cell animal in the same treatment group). Rats with fewer cells in the brain had a significantly smaller lesion volume on the day of cell transplantation than rats with more cells for all the animals studied (**D**, $^{\#}P<0.01$, fewer-cell animal versus more-cell animal). However, there was no significant difference in lesion reduction during the observation period between the animals with fewer- and more-cells (**E** and **F**).

the day of cell transplantation among treatment groups, $P > 0.87$). Rats with fewer cells in the brain had significantly smaller lesion volume on the day of cell transplantation than rats with more cells for all animals studied (Figure 3D, $P < 0.01$). However, there was no significant difference in T2 lesion reduction during the observation period between the animals with fewer and more cells (Figures 3E and 3F).

Correlation Analysis

The correlation between lesion volume on the day of cell transplantation and amount of cells detected in the brain (4 days after transplantation) was low for each treatment group ($R = 0.43$, 0.35, and 0.50 for the IV, IA, and IC group, respectively) and poor for both more- and fewer-cell groups ($R = 0.04$ and 0.06 for the more- and fewer-cell animal, respectively).

Mortality during Transplantation of NPCs

Rat deaths, which occurred during or immediately after cell delivery, were considered as transplantation-associated death, and those rats were counted for each group. IA delivery resulted in a higher mortality than IC and IV delivery ($P < 0.05$, IA versus IV). Forty-one percent of animals died from IA, as compared with 17% with IC and only 8% from IV administration. Mortality for the same rats with 2-h MCAo alone was about 10%.

In addition to death resulting from cell injection, some rats died during the following night or during MRI scans after cell transplantation in each treatment group ($n = 4$, 2, and 2 for IA, IC, and IV, respectively), and death of these rats was not considered as transplantation-associated death.

Discussion

The effects of delivery routes on the process of grafting NPCs into ischemic rat brain have been noninvasively and dynamically investigated using MRI. By monitoring engraftment *in vivo*, we show that MRI can visualize differences in migration and distribution of magnetically labeled NPCs transplanted into the host brain through the carotid artery, cisterna magna, and tail vein. IA administration produces a distinct difference from IC and IV administration regarding migration, distribution, extent, and amount of transplanted NPCs in the host brain. For each route of transplantation, the ischemic status of the brain at the time of cell transplantation seems to play a role in mediating the grafting process.

Cell-induced therapeutic benefits following stroke are evoked using various cellular delivery routes (Chopp and Li, 2002; Parr *et al*, 2007; Bacigaluppi *et al*, 2008). Among them, IV injection, a minimally invasive and clinically relevant technique, offers the most comfortable strategy for both subjects and operators. Some more invasive administration routes, such as IA and IC injection, are widely used in experimental studies and may be applied in future clinical practice (Li *et al*, 2001, Shen *et al*, 2006; Walczak *et al*, 2008; Zhang *et al*, 2004). We, therefore, assessed cell engraftment through these three delivery pathways.

Our data show that with all three delivery routes, transplanted NPCs can migrate to the ischemic brain and preferentially localize to the hemisphere ipsilateral to the ischemic lesion. While the cells appear in the lesion core area, numerous cells and cell clusters are usually detected nearby the lesion boundary, which provides a more supportive environment than the lesion core area for survival of transplanted NPCs (Savitz *et al*, 2004). In agreement with the previous finding that transplanted cells are attracted by and interact with tissue regions undergoing degeneration and reorganization (Modo *et al*, 2002), the injected cells are also found in the hemisphere contralateral to the ischemic lesion, although the amount is very small as compared with that in the ipsilateral hemisphere.

Our observations showed that delivery routes dramatically affected the migration and distribution of grafted cells. Despite an easy and safe pathway, IV administration led to delayed engraftment and lower numbers of grafted cells in the target brain than that by IC and IA administration (Figure 1), due to long-distance migration and a large proportion of cells trapped in the filtering organs (Kraitchman *et al*, 2005; Hauger *et al*, 2006; Parr *et al*, 2007). In contrast, IA administration could bring a large number of cells to the brain soon after transplantation (Figure 1) by bypassing the initial uptake by the systemic organs (Walczak *et al*, 2008). Since fewer cells were injected through the IC (1×10^5) than the IA and IV (1×10^6) routes in this study, this raises the possibility that the difference in the temporal profile of migration is due to the difference in the cell numbers injected. However, our data showed that even when more cells were infused through the tail vein, IV administration did not result in larger number and earlier arrival of grafted cells in the ischemic brain than IC administration (Figure 1). Therefore, delivery route is the determining factor for migration, not the cell numbers, at least in the range employed. It should be pointed out here that sensitivity of MRI to detect magnetically labeled cells depends on the MRI system and experimental setup (Magnitsky *et al*, 2005). Thus, very small cell clusters entering the ischemic brain may not be detected by MRI before a certain amount of these labeled cells has been accumulated, which could affect the estimate of the timing for grafted cells present in the brain. Our data suggest that under the current experimental conditions, initial accumulation of grafted cells within the target brain after IA administration was more rapid than IC and IV administration (overall route effect, $P < 0.01$). The distribution of grafts within the target

brain also reflected the effects of different administration routes. The distribution pattern after IA delivery appeared much more diffuse and widespread as compared with that after IC and IV delivery (comparing Figures 2D with Figures 2E and 2F), with grafted cells scattering discretely in an extensive range in the ischemic hemisphere, confirming previous reports (Walczak *et al*, 2008; Li *et al*, 2001). Although IA administration showed encouraging results, including earlier engraftment, more uniform and widespread distribution, and larger numbers of transplanted cells in the host brain than IC and IV administration, it was also accompanied by high mortality during cell delivery, consistent with a previous study (Walczak *et al*, 2008). The cause of animal death is probably due to further ischemia or thrombosis (Parr *et al*, 2007), as evidenced by significantly impeded cerebral blood flow (Walczak *et al*, 2008). In addition, severe edema induced by ischemia occurs between 24 and 48 h after MCAo for this stroke model, which increases intracranial pressure. Cell injection during this time with a volume of 1 ml suspension may worsen the situation and lead to high mortality. Further protocol optimization for cell administration is apparently needed.

As shown previously, particular locations in the brain selected for cell injection after stroke are subsequently associated with different functional benefits (Modo *et al*, 2002; Mochizuki *et al*, 2008), suggesting that different sites of transplantation may have their own value, and the type of functional recovery is affected by the localization of grafted cells within the brain (Modo *et al*, 2002; Roitberg, 2004). In addition, functional outcome after cell-based therapy is dose-dependent and a certain amount of grafted cells is necessary to significantly attenuate the functional deficits induced by ischemic injury (Chen *et al*, 2001). After systemic administration, the majority of transplanted cells home into the hemisphere ipsilateral to the ischemic lesion and evoke antiapoptotic and restorative effects, such as angiogenesis and neurogenesis (Chopp and Li, 2002). However, the exact localization of exogenous cells within the target brain after systemic transplantation cannot be controlled even though homing tendency to the ischemic lesion is expected, unless an invasive implantation, such as intracerebral injection (Chen *et al*, 2000; Zhao *et al*, 2002; Chen *et al*, 2008), is used. Our data indicate that IA delivery provides a wider distribution and larger number of grafted cells in the target brain than that by IC and IV delivery (Figure 1). These characteristics with IA administration may contribute in part to the observation that similar functional improvement after stroke, as measured by adhesive-removal test and neurological severity scores, can be achieved by IA injection (Li *et al*, 2001) with a lower dose of bone marrow stromal cells (2×10^6) than IV injection (Li *et al*, 2002) (3×10^6). Although functional recovery after cell transplantation has been shown in the previous studies using various cellular delivery routes and treatment protocols (Parr *et al*, 2007; Bacigaluppi *et al*, 2008), outcomes associated with the distribution and numbers of grafted cells in the target brain require further investigation.

The precise mechanism by which the transplanted cells are guided to the site of damaged tissue remains unknown, but the brain expresses chemotactic signals in response to ischemic injury that attract the cells and direct their migration to the damaged areas (Chopp and Li, 2002; Magnitsky *et al*, 2005; Shyu *et al*, 2006; Bacigaluppi *et al*, 2008). At the molecular level, matrix metalloproteinases (Wang *et al*, 2006; Lee *et al*, 2006) and the SDF-1/CXCR4 system (Wang *et al*, 2008) are involved in the directed cell migration. Our MRI observations show that whichever route of cell administration is chosen (IA, IC, or IV), NPCs have the capacity to migrate to the brain lesion area, once again providing evidence to support the concept that chemoattractive gradient released in the site of brain lesion leads to selective and specific homing of transplanted cells in the brain area suffering ischemic injury. Therefore, the status of the ischemic brain may play a critical pathobiological role to mediate the cell grafting process. Our measurements showed that a smaller lesion on the day of cell transplantation was significantly associated with fewer cells detected in the brain (Figure 3D, $P < 0.01$). These data suggest that stroke severity, such as ischemic lesion volume, affects the grafting process. However, there was no strong correlation between ischemic lesion volume on the day of cell transplantation and the amount of cells detected in the brain for each treatment group, for both the more- and fewer-cell group, indicating that cells present in the brain are not proportionally recruited by bigger lesions. As noted in the previous section, the amount of grafted cells in the brain varied greatly from animal to animal, even in the same treatment group. This broad variance in cerebral engraftment may be explained by heterogenous timing and pattern of pathophysiological changes after stroke for individual subjects (Walczak *et al*, 2008). But it was worth noting that in each treatment group, some animals had very few cells (less than 20 pixels with hypo-intensity on 3D MRI) as compared with others. These animals were considered as a specific group (fewer-cell animal; Figure 3). The degree of ischemic injury for these animals on the day of treatment was analyzed and compared with that of others. Our finding on the relationship between lesion volume at the time of cell transplantation and the amount of grafted cells detected in the brain, suggests the existence of a threshold for the spatial extent of ischemic injury at the time of treatment above which the signal or chemoattractive gradient released by ischemic lesion may better guide the grafted cells to the damaged areas. Cell transplantation executed at time points other than 24 h after MCAo may evoke different response of ischemic brain.

We are aware of limitations in our study. First, sensitivity of MRI to detect magnetically labeled cells is affected by a number of factors, including the hardware and software of MRI setup (Magnitsky *et al*, 2005). Therefore, our imaging measurements may not be sensitive enough to detect single cells or tiny cell clusters, which migrate to the host brain. Second, the degree of signal reduction in a local area relies on the concentration of SPIO or the size of the cell cluster. We used the same threshold to identify the volume of SPIO-induce signal reduction, which could underestimate the amount of grafted cells in the brain, especially for the IA group, since areas with signal alteration result from many small cell clusters, which might be excluded. Finally, hypo-intense areas on 3D MRI may include phagocytized PB-positive cells even though this effect is small on our study due to a short period after cell transplantation (4 days). However, our goal was to show the differences in migration and distribution following different cell delivery routes under the same experimental condition rather than to determine the minimum cell detection or quantify the grafted cells. The major characteristics for each route of cell engraftment seen on tissue slices were reflected on 3D MRI. As shown in Figure 2, more details depicted by *ex vivo* images than *in vivo* images did not change the fundamental picture. As an indirect technique, MRI at this time cannot provide accurate measurement of the amount of grafted cells in the target tissue (Liu and Frank, 2009). The volume of signal reduction on 3D MRI only provides a semi-quantitative assessment.

In summary, IA administration after transient MCAo shows significantly increased migration, a far more diffuse distribution pattern, and a larger number of transplanted NPCs in the target brain than IC or IV administration. However, high mortality with IA delivery poses a serious concern for using this route of administration. Further studies are clearly warranted before this strategy can be recommended for patients. Animals with smaller lesions (less than 10% of brain volume) on T2 map at the time of transplantation (24 h after MCAo) have fewer grafted cells into the parenchyma.

Disclosure/conflicts of Interest

The authors declare no conflict of interest.

References

Arbab AS, Pandit SD, Anderson SA, Yocum GT, Bur M, Frenkel V, Khuu HM, Read EJ, Frank JA (2006) Magnetic resonance imaging and confocal microscopy studies of magnetically labeled endothelial progenitor cells trafficking to sites of tumor angiogenesis. *Stem Cells* 24:671–8

Arbab AS, Yocum GT, Kalish H, Jordan EK, Anderson SA, Khakoo AY, Read EJ, Frank JA (2004) Efficient magnetic cell labeling with protamine sulfate complexed to ferumoxides for cellular MRI. *Blood* 104:1217–23

Amsalem Y, Mardor Y, Feinberg MS, Landa N, Miller L, Daniels D, Ocherashvilli A, Holbova R, Yosef O, Barbash IM, Leor J (2007) Iron-oxide labeling and outcome of transplanted mesenchymal stem cells in the infracted myocardium. *Circulation* 116:I38–45

Bacigaluppi M, Pluchino S, Martino G, Kilic E, Hermann DM (2008) Neural stem/precursor cells for the treatment of ischemic stroke. *J Neurol Sci* 265:73–7

Chen J, Li Y, Chopp M (2000) Intracerebral transplantation of bone marrow with BDNF after MCAo in rat. *Neuropharmacology* 39:711–6

Chen J, Li Y, Katakowski M, Chen X, Wang L, Lu D, Lu M, Gautam SC, Chopp M (2003*a*) Intravenous bone marrow stromal cell therapy reduces apoptosis and promotes endogenous cell proliferation after stroke in female rat. *J Neurosci Res* 73:778–86

Chen J, Li Y, Wang L, Zhang Z, Lu D, Lu M, Chopp M (2001) Therapeutic benefit of intravenous administration of bone marrow stromal cells after cerebral ischemia in rats. *Stroke* 32:1005–11

Chen J, Zhang ZG, Li Y, Wang L, Xu YX, Gautam SC, Lu M, Zhu Z, Chopp M (2003*b*) Intravenous administration of human bone marrow stromal cells induces angiogenesis in the ischemic boundary zone after stroke in rats. *Circ Res* 92:692–9

Chen JR, Cheng GY, Sheu CC, Tseng GF, Wang TJ, Huang YS (2008) Transplanted bone marrow stromal cells migrate, differentiate and improve motor function in rats with experimentally induced cerebral stroke. *J Anat* 213:249–58

Chopp M, Li Y (2002) Treatment of neural injury with marrow stromal cells. *Lancet Neurol* 1:92–100

Chu K, Kim M, Park KI, Jeong SW, Park HK, Jung KH, Lee ST, Kang L, Lee K, Park DK, Kim SU, Roh JK (2004) Human neural stem cells improve sensorimotor deficits in the adult rat brain with experimental focal ischemia. *Brain Res* 1016:145–53

Gao J, Dennis JE, Muzic RF, Lundberg M, Caplan AI (2001) The dynamic *in vivo* distribution of bone marrow-derived mesenchymal stem cells after infusion. *Cells Tissues Organs* 169:12–20

Garcia R, Aguiar J, Alberti E, de la Cuetaea K, Pavon N (2004) Bone marrow stromal cells produce nerve growth factor and glial cell line-derived neurotrophic factors. *Biochem Biophys Res Commun* 316:753–4

Hauger O, Frost EE, van Heeswijk R, Deminiere C, Xue R, Delmas Y, Combe C, Moonen CT, Grenier N, Bulte JW (2006) MR evaluation of the glomerular homing of magnetically labeled mesenchymal stem cells in a rat model of nephropathy. *Radiology* 238:200–10

Heohn M, Kustermann E, Blunk J, Wiedermann D, Trapp T, Wecker S, Focking M, Arnold H, Hescheler J, Fleischmann BK, Schwindt W, Buhrle C (2002) Monitoring of implanted stem cell migration *in vivo*: a highly resolved *in vivo* magnetic resonance imaging investigation of experimental stroke in rat. *Proc Natl Acad Sci USA* 99: 16267–72

Ishibashi S, Sakaguchi M, Kuroiwa T, Yamasaki M, Kanemura Y, Shizuko I, Shimazaki T, Onodera M, Okano H, Mizusawa H (2004) Human neural stem/progenitor cells, expanded in long-term neurosphere culture, promote functional recovery after focal ischemia in Mongolian gerbils. *J Neurosci Res* 78:215–23

Jiang Q, Zhang ZG, Ding GL, Silver B, Zhang L, Meng H, Lu M, Pourabdillah-Nejed DS, Wang L, Savant-Bhonsale S,

Li L, Bagher-Ebadian H, Hu J, Arbab AS, Vanguri P, Ewing JR, Ledbetter KA, Chopp M (2006) MRI detects white matter reorganization after neural progenitor cell treatment of stroke. *Neuroimage* 32:1080–9

Kraitchman DL, Tatsumi M, Gilson WD, Ishimori T, Kedziorek D, Walczak P, Segars WP, Chen HH, Fritzges D, Izbudak I, Young RG, Marcelino M, Pittenger MF, Solaiyappan M, Boston RC, Tsui BM, Wahl RL, Bulte JW (2005) Dynamic imaging of allogeneic mesenchymal stem cells trafficking to myocardial infarction. *Circulation* 112:1451–61

Lee SR, Kim HY, Rogowska J, Zhao BO, Bhide P, Parent JM, Lo EH (2006) Involvement of matrix metalloproteinase in neuroblast cell migration from the subventricular zone after stroke. *J Neurosci* 26:3491–5

Li L, Jiang Q, Ding GL, Zhang L, Zhang ZG, Ewing JR, Knight RA, Soltanian-Zadeh H, Chopp M (2005) MapISODATA demarcates regional response to combination rt-PA and 7E3 F(ab')$_2$ treatment of embolic stroke in the rat. *J Magn Reson Imaging* 21:726–34

Li Y, Chen J, Chen XG, Wang L, Gautam SC, Xu YX, Katakowski M, Zhang LJ, Lu M, Janakiraman N, Chopp M (2002) Human marrow stromal cell therapy for stroke in rat: neurotrophins and functional recovery. *Neurology* 59:514–23

Li Y, Chen J, Wang L, Lu M, Chopp M (2001) Treatment of stroke in rat with intracarotid administration of marrow stromal cells. *Neurology* 56:1666–72

Li Y, McIntosh K, Chen J, Zhang C, Gao Q, Borneman J, Raginski K, Mitchell J, Shen L, Zhang J, Lu D, Choop M (2006) Allogeneic bone marrow stromal cells promote glial–axonal remodeling without immunologic sensitization after stroke in rats. *Exp Neurol* 198:313–25

Liu W, Frank JA (2009) Detection and quantification of magnetically labeled cells by cellular MRI. *Eur J Radiol* 70:258–64

Liu XS, Zhang ZG, Zhang RL, Gregg S, Morris DC, Wang Y, Chopp M (2007) Stroke induces gene profile changes associated with neurogenesis and angiogenesis in adult subventricular zone progenitor cells. *J Cereb Blood Flow Metab* 27:564–74

Luskin MB, Zigova T, Soteres BJ, Stewart RR (1997) Neuronal progenitor cells derived from the anterior subventricular zone of the neonatal rat forebrain continue to proliferate *in vitro* and express a neuronal phenotype. *Mol Cell Neurosci* 8:351–66

Magnitsky S, Watson DJ, Walton RM, Pickup S, Bulte JW, Wolfe JH, Poptani H (2005) *In vivo* and *ex vivo* MRI detection of localized and disseminated neural stem cell grafts in the mouse brain. *Neuroimage* 26:744–54

Mochizuki N, Takagi N, Kurokawa K, Onozato C, Moriyama Y, Tanonaka K, Takeo S (2008) Injection of neural progenitor cells improved learning and memory dysfunction after cerebral ischemia. *Exp Neurol* 211:194–202

Modo M, Stroemer RP, Tang E, Patel S, Hodges H (2002) Effects of implantation site of stem cell grafts on behavioral recovery from stroke damage. *Stroke* 33:2270–8

Ohta M, Suzuki Y, Noda T, Ejiri Y, Dezawa M, Kataoka K, Chou H, Ishikawa N, Matsumoto N, Iwashita Y, Mizuta E, Kuno S, Ide C (2004) Bone marrow stromal cells infused into the cerebrospinal fluid promote functional recovery of the injured rat spinal cord with reduced cavity formation. *Exp Neurol* 187:266–78

Parr AM, Tator CH, Keating A (2007) Bone marrow-derived mesenchymal stromal cells for the repair of central nervous system injury. *Bone Marrow Transplantation* 40:609–19

Roitberg B (2004) Transplantation for stroke. *Neurol Res* 26:256–64

Savitz SI, Dinsmore JH, Wechsler LR, Rosenbaum DM, Caplan LR (2004) Cell therapy for stroke. *NeuroRx* 1:406–16

Shen LH, Li Y, Chen J, Zhang J, Vanguri P, Borneman J, Chopp M (2006) Intracarotid transplantation of bone marrow stromal cells increases axon-myelin remodeling after stroke. *Neuroscience* 137:393–9

Shyu WC, Lee YJ, Liu DD, Lin SZ, Li H (2006) Homing genes, cell therapy and stroke. *Front Biosci* 11:899–907

Zhang Z, Jiang Q, Jiang F, Ding G, Zhang R, Wang L, Zhang L, Robin AM, Katakowski M, Chopp M (2004) *In vivo* magnetic resonance imaging tracks adult neural progenitor cell targeting of brain tumor. *Neuroimage* 23:281–7

Zhao LR, Duan WM, Reves M, Keene CD, Verfailie CM, Low WC (2002) Human bone marrow stem cells exhibit neural phenotypes and ameliorate neurological deficits after grafting into the ischemic brain of rats. *Exp Neurol* 174:11–20

Walczak P, Zhang J, Gilad AA, Kedziorek DA, Ruiz-Cabello J, Young RG, Pittenger MF, van Zijl PC, Huang J, Bulte JW (2008) Dual-modality monitoring of targeted intraarterial delivery of mesenchymal stem cells after transient ischemia. *Stroke* 39:1569–74

Wang L, Zhang ZG, Zhang RL, Gregg SR, Hozeska-Solgot A, LeTourneau Y, Wang Y, Choop M (2006) Matrix metalloproteinase 2 (MMP2) and MMP9 secreted by erythropoietin-activated endothelial cells promote neural progenitor cell migration. *J Neurosci* 26:5996–6003

Wang Y, Deng Y, Zhou GQ (2008) SDF-1alpha/CXCR4-mediated migration of systemically transplanted bone marrow stromal cells towards ischemic brain lesion in a rat model. *Brain Res* 1195:104–12